Accuracy and Convergence of the Time Domain Wave Equation Methods

Natalia K. Nikolova, Yotka S. Rickard, and Ying Li

Department of Electrical and Computer Engineering, McMaster University
Hamilton, Ontario, L8S 4K1, Canada

***Abstract* — Time-domain electrodynamics is formally described either by Maxwell's equations or by the wave equation. In the former case, the system state is described by the field vectors E and H, while the electromagnetic potentials are the usual choice in the latter case. Here, we investigate the accuracy and the convergence of the time domain wave equation method based on the scalar wave potentials in the treatment of edges and corners. Comparisons are provided with the commonly used finite-difference time domain (FDTD) method based on Yee's discretization and with the time domain transmission-line matrix (TLM) method.**

Keywords – Wave equation, Electromagnetic potentials, FDTD methods.

I. INTRODUCTION

Ever since Heaviside (in 1885) [1] and Hertz (in 1884) independently stated the "duplex" equations (now called Maxwell's equations) as the basic equations of electrodynamics, two distinct views have existed on what the primary and the secondary electromagnetic quantities are. The orthodox view due to Maxwell [2] and Lorenz [3][4], points to the four-potential $(\mathbf{A},\phi)$ as the primary (energy-related) quantity, while the field vectors **E** and **B** (or **D** and **H**) are simply derivatives. This view is dominant in theoretical and quantum physics. On the other hand, the Hertz-Heaviside view adopts the force-related vectors **E** and **B** as primary, while the potentials are an occasional computational facility.[1] The two mathematical models yield identical results in *almost* all cases. Where they fail to agree, curious (some yet unsolved) paradoxes occur.

In time-domain numerical electromagnetics, the force-field view is prevalent, and only few algorithms exploiting potential concepts exist. For example, in the integral-equation techniques for radiation/scattering problems, the vector potentials are computed as the integrals over actual and/or equivalent sources.

Also, there is no popular partial differential equation technique based on the electromagnetic potentials. This contradicts the opinion that they are convenient computationally. Indeed, two factors have already been pointed out [5][6], which have prevented their adoption: (a) there are modest savings in computer time (not in memory) when using the three-component **A** vector in comparison with a field-based computation such as the FDTD algorithm; (b) there are difficulties in defining the boundary conditions for the vector potentials. With respect to the latter factor, it may be more convenient to use the vector wave equation with the electric field **E** [7] rather than with **A**: the computational resources are the same but the implementation of the boundary conditions is simpler. We note, however, that in certain applications, it is the vector potential that we are interested in, not the field vectors. While we can easily derive the field vectors from a vector-potential solution, the reverse is not true.

In this work, we focus on the accuracy of the time-domain wave potential (TDWP) technique [8][9], which is, to our knowledge, the most computationally efficient wave-equation technique. We compare it with other popular time domain techniques, the FDTD and the TLM methods. The accuracy is investigated through the computation of the resonant frequencies of rectangular cavities, in which metallic objects with 90-degree edges and knife edges are present. We use the test structures proposed in [11], and analyze them with increasingly finer mesh. We estimate the accuracy at each grid cell size through a convergence error and an extrapolated value of the resonant frequency.

II. THE TDWP APPROACH

The TDWP technique uses a pair of collinear vector potentials: the magnetic potential $\mathbf{A}_\mu = \hat{\mathbf{c}}A_\mu$ (measured

[1] Sir Oliver Heaviside considered the vector and scalar potentials [1] "… powerful aids to obscuring and complicating the subject, and hiding from view useful and sometimes important relations."

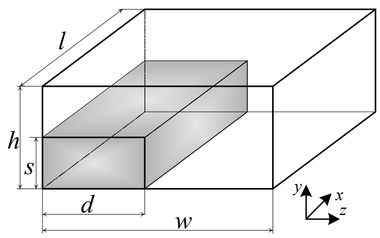

Fig. 1. Cavity with a 90° edge: $l = 14$ mm, $w = 10$ mm, $h = 6$ mm, $d = 5$ mm, $s = 3$ mm.

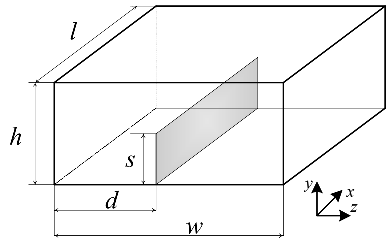

Fig. 2. Cavity with a knife edge: $l = 30$ mm, $w = 20$ mm, $h = 10$ mm, $d = 10$ mm, $s = 5$ mm.

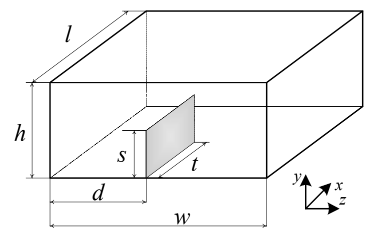

Fig. 3. Cavity with a knife-edge corner: $l = 10$ mm, $w = 6$ mm, $h = 2$ mm, $d = 3$ mm, $s = 1$ mm, $t = 5$ mm.

in *amperes*) and the electric potential $\mathbf{F}_\varepsilon = \hat{\mathbf{c}} F_\varepsilon$ (measured in *volts*). In [9], the direction of the vector potentials $\hat{\mathbf{c}}$ (the distinguished or preferred axis) is fixed throughout the computational volume, for which the approach is named *uniaxial*. This is in contrast with the technique considered in [8], where the preferred axis changes in the sub-domains of the computational volume. The uniaxial algorithm is simpler to implement. It transforms equivalently the secondary (induced by the field) current densities at metallic edges and material nonuniformities, when these currents are orthogonal to the preferred axis. The equivalent current densities are co-parallel with the preferred axis.

In both TDWP algorithms, two scalar variables (the wave potentials A_μ and F_ε) describe the field in space and time. They satisfy two wave equations, which, in the uniaxial algorithm [9], are coupled at material interfaces whose unit normal is orthogonal to the preferred axis, as well as at metallic edges, which are orthogonal to the preferred axis. In the original TDWP algorithm [8], the coupling occurs at the mutual boundaries of the sub-domains. With finite differences, both algorithms require two-thirds of the computer memory and time required by Yee's FDTD algorithm [8][9].

We briefly mention that the finite-difference treatment of the vector wave equation for the three-component magnetic vector potential **A** is also possible, see, e.g., [5]. The savings in computational time are modest compared to Yee's FDTD algorithm; however, the technique yields the space-time dependence of the **A** vector directly. We note that the computation of **A** from **E** and **H** requires the solution of an additional 3-D partial differential equation.

III. Accuracy and Convergence Analysis

It has already been indicated that the uniaxial TDWP method exhibits excellent accuracy even with coarser grids [10]. Specifically, this observation was made for the case when the two scalar wave potential equations are decoupled. The theoretical reasoning given in [10] is based on the fact that the wave potentials are not singular in the vicinity of metallic edges and corners. This result, however, has never been investigated numerically with sufficient thoroughness, especially in the case when the two wave equations are coupled.

We calculate the resonant frequencies of the cavities in Figures 1, 2, and 3, using the TDWP techniques, as well as with an in-house FDTD simulator. The TLM results are taken from [11]. These results have been verified and complemented by additional results for even finer TLM grids with the commercial TLM solver MEFiSTo-3D [12].

In the TDWP simulations, in all three cases we employ the potential pair $\hat{\mathbf{x}}(A_\mu, F_\varepsilon)$. This makes the analysis of the first two structures simple: the wave potentials A_μ (describing TM_x modes) and F_ε (describing TE_x modes) are decoupled and can be analyzed independently. It also saves time: after the first simulation with the coarsest grid, we establish that in both structures the dominant resonant mode is due to F_ε (the TE_x mode). From this point on, the simulations with finer grids are carried out only for the F_ε wave potential: the computational resources (time and memory) are about one-third of those required by Yee's FDTD. In the case of the knife-edge corner, the wave potentials are coupled at the vertical (along y) edge of the knife, and the two wave equations run simultaneously.

In all simulations, field values are recorded at random locations inside the cavity different from the locations of the sources. The recorded waveforms are then processed with the fast Fourier transform (FFT). The maximum spectral component at the lowest-frequency is located, and this frequency is recorded as the computed dominant-mode resonance f_r. It is desirable to make the FFT error, which is due to the truncation of the time sequence, independent of the discretization step. For that, the number of recorded time samples increases inverse proportionally to the size of the grid cell Δh (which is also proportional to the discretization step in time Δt). In all cases, the longest time sample (for the finest grid) is $150000\Delta t$. The ratio $q = \Delta h/(c\Delta t)$ is set to 2 in the TDWP and the FDTD computations, while with MEFiSTo-3D, q is left at a default value of 1.9986.

TABLE I
RESONANT FREQUENCY AND CONVERGENCE ERROR OF THE CAVITY WITH A 90°-EDGE

Δh [mm] (size in Δh)	f_r [GHz] (Convergence Error, *e* [%])		
	FDTD	TLM	TDWP
1.0 ($14\times6\times10$)	16.96825 (NA)	16.9005 (NA)	16.96825 (NA)
0.5 ($28\times12\times20$)	17.09120 (0.719)	17.0653 (0.966)	17.09297 (0.729)
0.25 ($56\times24\times40$)	17.14210 (0.297)	17.1281 (0.367)	17.13854 (0.266)
0.125 ($112\times48\times80$)	17.16010 (0.105)	17.1523 (0.141)	17.15292 (0.084)
$\to 0$	**17.1713**	**17.1711**	**17.1585**

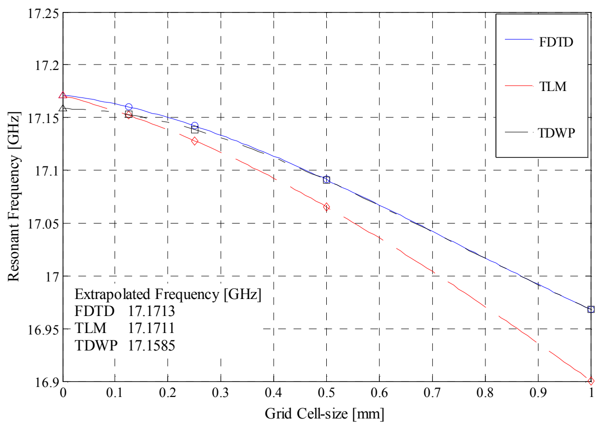

Fig. 4. Resonant frequency of the cavity with a 90° edge: FDTD – solid line, TLM – dash line, TDWP – dash-dot line. Extrapolated frequencies are marked by triangles.

The convergence rate of each technique is represented in terms of the relative convergence error. This is the relative difference between the resonant frequencies, which are calculated with two consecutive mesh sizes, Δh_{n-1} and Δh_n:

$$e_n = \frac{\left| f_r(\Delta h_n) - f_r(\Delta h_{n-1}) \right|}{f_r(\Delta h_n)} \times 100,\ \%\,. \qquad (1)$$

We also compute a reference resonant frequency by a spline extrapolation[2] of the dependence $f_r(\Delta h)$: $f_r^{ref}(\Delta h = 0) = \lim_{\Delta h \to 0} f_r(\Delta h)$. Each technique has its own reference f_r^{ref}, since there is no common reference value that we could use, e.g., an analytical solution. The FDTD, TLM, and TDWP references provide some measure of the agreement among the three approaches.

A. Cavity with a 90-degree edge

The results for the cavity shown in Fig. 1 are summarized in Table I. The resonant frequencies obtained by the TDWP technique are practically identical to those generated with the FDTD method. All techniques seem to exhibit a comparable (quadratic) convergence rate, which is to be expected from second-order accurate finite-difference schemes, see the curves plotted in Fig. 4. We should note that the differences between the three curves are indeed minor: less than 0.1 % at each cell size. The scale of the ordinate is very fine for better display of the convergence rate.

[2] We use the cubic spline in MATLAB [13].

TABLE II
RESONANT FREQUENCY AND CONVERGENCE ERROR OF THE CAVITY WITH A KNIFE EDGE

Δh [mm] (size in Δh)	f_r [GHz] (Convergence Error, *e* [%])		
	FDTD	TLM	TDWP
2.5 ($12\times4\times8$)	7.53498 (NA)	7.30429 (NA)	7.53510 (NA)
1.0 ($30\times10\times20$)	7.74330 (2.69)	7.65399 (4.569)	7.74304 (2.69)
0.5 ($60\times20\times40$)	7.81200 (0.879)	7.76706 (1.456)	7.81139 (0.875)
0.25 ($120\times40\times80$)	7.84800 (0.459)	7.82339 (0.720)	7.84737 (0.458)
0.125 ($240\times80\times160$)	7.86500 (0.216)	7.85009 (0.340)	7.86336 (0.203)
$\to 0$	**7.8804**	**7.8749**	**7.8764**

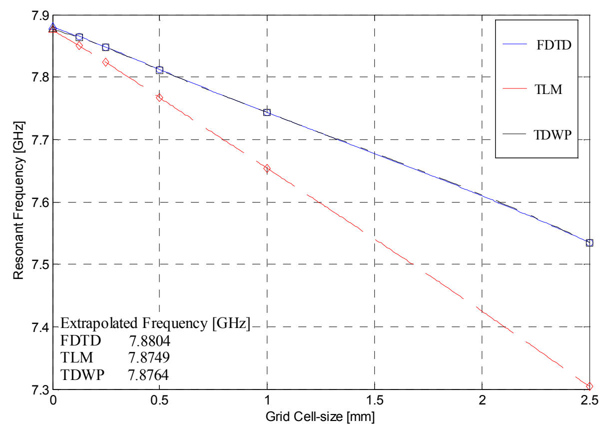

Fig. 5. Resonant frequency of the cavity with a knife edge: FDTD – solid line, TLM – dash line, TDWP – dash-dot line. Extrapolated frequencies are marked by triangles.

B. Cavity with a knife edge

Table II and Fig. 5 summarize the results for the resonant frequency of the structure shown in Fig. 2. The conclusions are basically the same as with the previous example. Here, the reference resonant frequencies obtained by the three methods agree remarkably well.

C. Cavity with a knife edge 90-degree corner

The corners of infinitesimally thin plates are a challenge for all numerical solvers because of the singularity of four out of the six field components in its

TABLE III
RESONANT FREQUENCY AND CONVERGENCE ERROR OF THE CAVITY WITH A KNIFE EDGE CORNER

Δh [mm] (size in Δh)	f_r [GHz] (Convergence Error, e [%])		
	FDTD	TLM	TDWP
1.0 ($10\times2\times6$)	24.9434 (NA)	23.6396 (NA)	25.6589 (NA)
0.5 ($20\times4\times12$)	26.2390 (4.938)	25.8587 (8.582)	26.5653 (3.412)
0.25 ($40\times8\times24$)	26.7940 (2.071)	26.6537 (2.983)	26.9507 (1.430)
0.125 ($80\times16\times48$)	27.0437 (0.932)	26.9862 (1.232)	27.1283 (0.655)
0.0625 ($160\times32\times96$)	27.1708 (0.459)	27.1336 (0.543)	27.2087 (0.295)
$\rightarrow 0$	**27.3060**	**27.2664**	**27.2805**

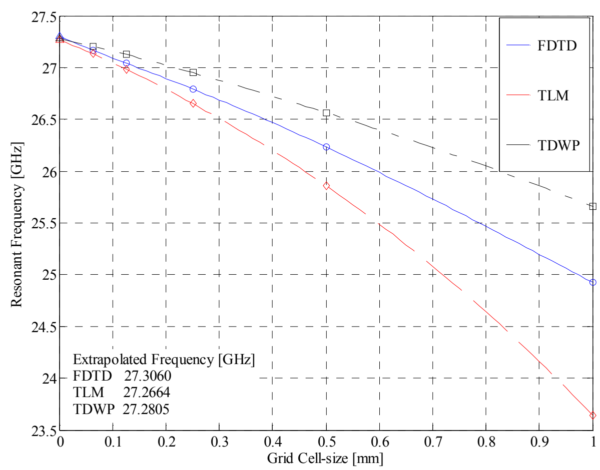

Fig. 6. Resonant frequency of the cavity with a knife edge corner: FDTD – solid line, TLM – dash line, TDWP – dash-dot line. Extrapolated frequencies are marked by triangles.

vicinity. As seen from Table III and Fig. 6, indeed, the differences between the results of the three techniques are largest in this example. The TDWP technique still exhibits remarkable convergence.

IV. CONCLUSION

We presented recent results from the investigation of the accuracy and the convergence of the uniaxial time domain wave potential (TDWP) algorithm. The convergence is estimated with respect to the size of the (uniform) grid cell. The results are compared with those generated by common time domain techniques: the FDTD and the TLM methods. We conclude that the wave potential technique has equivalent or better convergence and accuracy compared to the above techniques. The convergence rate is nearly identical or slightly better in the case of 90° and knife edges. It is notably better in the case of corners. In all cases and with all three techniques, no special corrections were used to account for the field singularity at the metallic edges and corners.

This investigation is in progress, and it still has to address a number of important issues. (A) Additional experiments are necessary with regard to both concave and convex edges and corners. (B) In the physics community, the time domain vector-potential technique, which solves the vector wave equation directly for the magnetic vector potential **A** [5], is of greater interest, despite the fact that its computational requirements are larger (comparable to those of the TDWP algorithm). Therefore, this investigation has to address its accuracy, and compare it with that of the TDWP technique. (C) Grid-dispersion errors are expected to be of the same order as the FDTD method; however, this is still to be verified experimentally. (D) A similar comparison is due in the case of dielectric interfaces and corners.

REFERENCES

[1] O. Heaviside, *Electromagnetic Theory*, vol. 1, London: Ernest Benn Limited, 1893, pp. iii-iv, and pp. 20-125 (Chapter II).

[2] J.C. Maxwell, *A Treatise on Electricity and Magnetism*, New York: Dover Publications, Inc., 1954.

[3] L. Lorenz, "On the identity of the vibrations of light with electrical currents," *Philosophical Magazine and Journal of Science*, vol. 34, pp. 287-301, July-Dec. 1867.

[4] R. Nevels and C.-S. Shin, "Lorenz, Lorentz, and the gauge," *IEEE Antennas and Propagation Magazine*, vol. 43, No. 3, June 2001, pp. 1-37.

[5] N.K. Georgieva and E. Yamashita, "Time-domain vector-potential analysis of transmission line problems," *IEEE Trans. Microwave Theory Tech.*, vol. 46, No. 4, pp. 404-410, April 1998.

[6] N.K. Georgieva, *Studies in Numerical Time-domain Methods for the Analysis of Transient Electromagnetic Fields*, Ph.D. Thesis, University of Electro-communications, Tokyo, 1997.

[7] P. Aoyagi, J.-F. Lee, and R. Mittra, "A hybrid Yee algorithm/scalar wave equation approach," *IEEE Trans. Microwave Theory Tech.*, vol. 41, pp. 1593–1600, Sept. 1993.

[8] N.K. Georgieva, "Construction of solutions to electro-magnetic problems in terms of two collinear vector potentials," *IEEE Trans. Microwave Theory Tech.*, vol. 50, pp. 1950-1959, Aug. 2002.

[9] N.K. Nikolova, "A uniaxial approach to time-domain computations using EM potentials," *Int. J. of Numerical Modelling: Electronic Networks, Devices and Fields*, vol. 17, pp. 269-284, May/June 2004.

[10] N.K. Georgieva and W.S. Weiglhofer, "Electromagnetic vector potentials in isotropic nonhomogeneous materials: mode equivalence and scalarization," *IEE Proc.-Microw. Antennas Propag.*, vol. 150, No. 3, pp. 164-170, June 2003.

[11] H. Du, P.M. So and W.J.R. Hoefer, "Generalized and numerically robust singularity correction in TLM models of electromagnetic fields," *19th Annual Review of Progress in Applied Computational Electromagnetics*, pp. 383-389, 2003.

[12] MEFiSTo-3D® Pro v. 4.0, Faustus Scientific.

[13] MATLAB® v. 6.5.1 Release 13, The Mathworks.